THE JOURNAL OF BIOLOGICAL CHEMISTRY VOL. 291, NO. 31, pp. 16048–16058, July 29, 2016

Krüppel-like Factor 3 (KLF3/BKLF) Is Required for Widespread Repression of the Inflammatory Modulator Galectin-3 (*Lgals3*)*

Received for publication, January 24, 2016, and in revised form, May 22, 2016 Published, JBC Papers in Press, May 24, 2016, DOI 10.1074/jbc.M116.715748

Alexander J. Knights[‡1], Jinfen J. Yik[‡1], Hanapi Mat Jusoh[§2], Laura J. Norton[‡1], Alister P. W. Funnell[‡], Richard C. M. Pearson[‡], Kim S. Bell-Anderson[¶], Merlin Crossley[‡], and Kate G. R. Quinlan[‡3]

From the [‡]School of Biotechnology and Biomolecular Sciences, University of New South Wales, Sydney, New South Wales 2052 and the [§]School of Molecular Bioscience and [¶]Charles Perkins Centre, School of Life and Environmental Sciences, University of Sydney, Sydney, New South Wales 2006, Australia

The *Lgals3* gene encodes a multifunctional β-galactoside-binding protein, galectin-3. Galectin-3 has been implicated in a broad range of biological processes from chemotaxis and inflammation to fibrosis and apoptosis. The role of galectin-3 as a modulator of inflammation has been studied intensively, and recent evidence suggests that it may serve as a protective factor in obesity and other metabolic disorders. Despite considerable interest in galectin-3, little is known about its physiological regulation at the transcriptional level. Here, using knockout mice, chromatin immunoprecipitations, and cellular and molecular analyses, we show that the zinc finger transcription factor Krüppel-like factor 3 (KLF3) directly represses galectin-3 transcription. We find that galectin-3 is broadly up-regulated in KLF3-deficient mouse tissues, that KLF3 occupies regulatory regions of the *Lgals3* gene, and that KLF3 directly binds its cognate elements (CACCC boxes) in the galectin-3 promoter and represses its activation in cellular assays. We also provide mechanistic insights into the regulation of *Lgals3*, demonstrating that C-terminal binding protein (CtBP) is required to drive optimal KLF3-mediated silencing. These findings help to enhance our understanding of how expression of the inflammatory modulator galectin-3 is controlled, opening up avenues for potential therapeutic interventions in the future.

Lectin, galactoside-binding, soluble 3 (*Lgals3*) encodes galectin-3, a 35-kDa protein noted for its diverse molecular roles in pre-mRNA splicing (1), macrophage activation (2), tumorigenesis (3), apoptosis (4), and other important cellular processes. Recent studies at the level of the whole organism have shown galectin-3 to be important in heart disease and fibrosis (5, 6), and it is now used routinely as a prognostic biomarker in heart failure patients (7). Furthermore, galectin-3 is an essential regulator of inflammation in metabolic tissues, able to protect pancreatic β cells from interleukin 1β cytotoxicity (8) and to neutralize inflammatory factors known as advanced glycation end products (9). However, despite our extensive knowledge of its significance in various biological processes and disease states, little is known about how the expression of *Lgals3* is controlled. Developing a more thorough understanding of how *Lgals3* is regulated should provide important information on the biological pathways upon which it operates and may ultimately provide strategies for therapeutic interventions.

While studying genetically modified mice with a mutation in the gene encoding the zinc finger transcription factor Krüppel-like factor 3 (KLF3/BKLF), we noted that the *Lgals3* gene was consistently up-regulated. KLF3 is one of 18 members of the Krüppel-like factor (KLF)[4] family of DNA-binding proteins, responsible for controlling gene expression at the transcriptional level in a diverse range of biological settings. All KLF family members possess three evolutionarily conserved Cys^2-His^2 zinc fingers that facilitate binding to CACCC boxes and related GC-rich motifs in regulatory regions of DNA (10, 11). KLFs are able to function as potent activators or repressors of transcription through interaction with protein co-factors via their highly variable N-terminal functional domains. KLF4, for instance, has been shown to both silence and activate gene expression depending on promoter availability and the presence of specific co-factors (12, 13). Because of their inherent DNA-binding homology, KLFs are known to share target genes and operate within transcriptional networks (14). For instance, KLF feedback repression has been observed where KLF3 acts to silence a series of KLF1 target genes during erythropoiesis (15). KLF3 itself was first identified in a screen for factors in erythroid cells with homology to the DNA-binding domain of the founding family member KLF1 (16) but is now known to show a broad tissue expression profile (11). KLF3 is notable for being primarily a repressor of transcription. Upon binding control regions of its target genes, KLF3 recruits the co-repressor C-terminal binding protein (CtBP) via the N-terminal functional domain (17), which subsequently facilitates the assembly of a potent repressor complex of histone-modifying enzymes and other co-repressors to silence transcription (18, 19). Post-

* This work was supported by National Health and Medical Research Council Grant APP1025877. The authors declare that they have no conflicts of interest with the contents of this article.
[1] Supported by Australian Postgraduate Awards.
[2] Supported by an Academic Training Scheme (SLAB) scholarship from the Malaysian Ministry of Higher Education.
[3] To whom correspondence should be addressed: School of Biotechnology and Biomolecular Sciences, University of New South Wales, Sydney, NSW 2052, Australia. Tel.: 61-2-9385-8586; E-mail: kate.quinlan@unsw.edu.au.

[4] The abbreviations used are: KLF, Krüppel-like factor; CtBP, C-terminal binding protein; MEF; murine embryonic fibroblast; scWAT, subcutaneous white adipose tissue; epiWAT, epididymal white adipose tissue; BAT, brown adipose tissue; ChIP-seq, ChIP sequencing; DNase-seq, DNase sequencing; BMDM, bone marrow-derived macrophage(s).

translational modifications of KLF3 by phosphorylation and sumoylation have also been implicated in enhancing its repressive activity (20, 21). KLF3 has been implicated in a host of biological roles spanning from the regulation of B cell development (22) and erythropoiesis (15) to adipogenesis (23, 24) and, more recently, in heart function (25).

Here we set out to assess whether *Lgals3* is a *bona fide* target of KLF3-mediated repression at the transcriptional level. We found that *Lgals3* is consistently up-regulated in mouse-derived cell lines lacking KLF3, prompting a more rigorous examination of *Lgals3* expression across KLF3-deficient tissues. *Lgals3* was found to be highly derepressed in both subcutaneous and visceral white adipose depots as well as in the heart and pancreas of *Klf3*$^{-/-}$ mice. Given its importance in fat homeostasis, closer examination of *Lgals3* deregulation in subcutaneous adipose tissue was undertaken by immunohistochemistry, illustrating a distinct up-regulation in both the adipocytes and stromal vascular compartment in the absence of KLF3. The ability of KLF3 to bind to regulatory elements within the *Lgals3* gene was confirmed by electrophoretic mobility shift assays and chromatin immunoprecipitation experiments, suggesting that KLF3 occupies *Lgals3* regulatory regions *in vivo*. We also demonstrated that KLF1-driven activation of *Lgals3* is suppressed with the addition of KLF3 and that CtBP participates in the mediation of repression. Together, these results represent the first evidence that *Lgals3* is a direct target of KLF3 binding and repression.

Interestingly, mice lacking *Lgals3* display increased fat mass and systemic inflammation (26–28), the inverse of the phenotype seen in *Klf3*$^{-/-}$ mice, which are obesity-resistant with reduced adiposity (23, 24). The observation that KLF3 directly represses the galectin-3 gene and that the two proteins play what are essentially opposing roles in metabolic homeostasis is consistent with contributing to a regulatory circuit that controls both inflammation and metabolism.

Results

Lgals3 Is Up-regulated in the Absence of KLF3—In studies of the role of KLF3 in hematopoiesis and red blood cell development, microarrays performed on Ter119^{+} fetal liver cells lacking KLF3 revealed that the *Lgals3* gene was consistently up-regulated in knockout animals (15). Because of the importance of galectin-3 in a number of biological settings, we undertook a fuller analysis of whether the expression of *Lgals3* was altered in a range of mouse tissues in the absence of KLF3. *Lgals3* mRNA levels were assessed in cultured murine embryonic fibroblasts (MEFs) as well as a series of primary tissues from wild-type and *Klf3*$^{-/-}$ mice by quantitative real-time PCR. In primary and immortalized *Klf3*$^{-/-}$ MEFs, *Lgals3* mRNA was up-regulated 4.7- and 4.3-fold, respectively, compared with wild-type expression (Fig. 1*A*). Importantly, *Lgals3* levels were also found to be elevated in a number of primary tissues dissected from KLF3-deficient mice (Fig. 1*B*). Derepression was most evident in *Klf3*$^{-/-}$ subcutaneous (6.7-fold) and epididymal (3.3-fold) white adipose depots and in the heart (6.6-fold) and pancreas (4.2-fold).

Following the demonstration that *Lgals3* is derepressed in *Klf3*$^{-/-}$ tissues at the mRNA level, we next sought to determine whether this up-regulation was reflected at the protein level. Whole cell protein extracts were prepared from wild-type and *Klf3*$^{-/-}$ fat depots and spleens, and the expression of galectin-3 protein was assessed by Western blotting (Fig. 1, *C–F*). Significant elevation of galectin-3 protein was evident in *Klf3*$^{-/-}$ white adipose depots, with up-regulation being 6.7-fold in subcutaneous white adipose tissue (scWAT) (Fig. 1*D*) and 7.6-fold in epididymal white adipose tissue (epiWAT) (Fig. 1*E*). Expression was also modestly but significantly up-regulated in the brown adipose tissue (BAT) (Fig. 1*C*) and spleen (Fig. 1*F*) of animals lacking KLF3 (3.5- and 2.4-fold, respectively). These observations correlate well with the degree of up-regulation observed at the transcript level and, together, point to widespread derepression of *Lgals3* in the absence of KLF3.

As galectin-3 expression was found to be markedly derepressed in *Klf3*$^{-/-}$ mouse adipose tissue at the mRNA and protein levels, we decided to determine in which specific cell types this was occurring using independent methodologies. We performed immunofluorescent staining of galectin-3 in scWAT (Fig. 2*A*). In accordance with mRNA and protein expression results, galectin-3 was found to be considerably up-regulated in *Klf3*$^{-/-}$ scWAT, as calculated by corrected total fluorescence (Fig. 2*B*). *Klf3*$^{-/-}$ scWAT in pairs 1 and 2 registered 9- and 10.5-fold up-regulation of galectin-3 expression, respectively. In addition to the examination of cellular galectin-3 levels, an *ex vivo* analysis of galectin-3 secretion from epiWAT explants was conducted by enzyme-linked immunosorbent assay, revealing 2.7-fold higher levels of secretion from *Klf3*$^{-/-}$ fat (Fig. 2*C*).

Closer inspection of the scWAT by immunofluorescence showed increased galectin-3 staining in both adipocytes and cells of the stromal vascular compartment (the non-adipocytes) in scWAT lacking KLF3 (Fig. 2*D*). To better quantify the differential expression of *Lgals3* in these subfractions of the scWAT, quantitative real-time PCR was conducted, confirming that *Lgals3* mRNA is significantly up-regulated in both the adipocytes (5-fold) and stromal vascular cells (3.8-fold) of *Klf3*$^{-/-}$ scWAT (Fig. 2*E*). Given that galectin-3 is important in macrophage activation (2) and that macrophages are an integral cell type of the stromal vascular compartment, we assessed *Lgals3* transcript levels in bone marrow-derived macrophages (Fig. 2*F*). We found that *Lgals3* expression is modestly but significantly elevated in the absence of KLF3 in these cells, showing a 1.4-fold up-regulation. Taken together, these results demonstrate that galectin-3 expression is significantly derepressed at both the mRNA and protein levels in several different cell types and tissues in mice lacking KLF3.

KLF3 Binds the Lgals3 Promoter—To investigate whether KLF3 regulates *Lgals3* expression directly, the ability of KLF3 to bind to the *Lgals3* locus was assessed. We first explored the mechanism by which KLF3 might directly repress *Lgals3* by focusing on the proximal promoter. Indeed, KLF3 has been shown in several previous cases to silence gene expression by directly binding to promoter elements through recognition of CACCC motifs and related GC-rich regions (15, 23, 29). We examined the sequence between −60 and +20 bp relative to the *Lgals3* transcription start site and observed several KLF3 consensus binding sites (16, 29) (shown as *boxes* in Fig. 3*A*). To assess whether KLF3 could bind these sites *in vitro*, we prepared

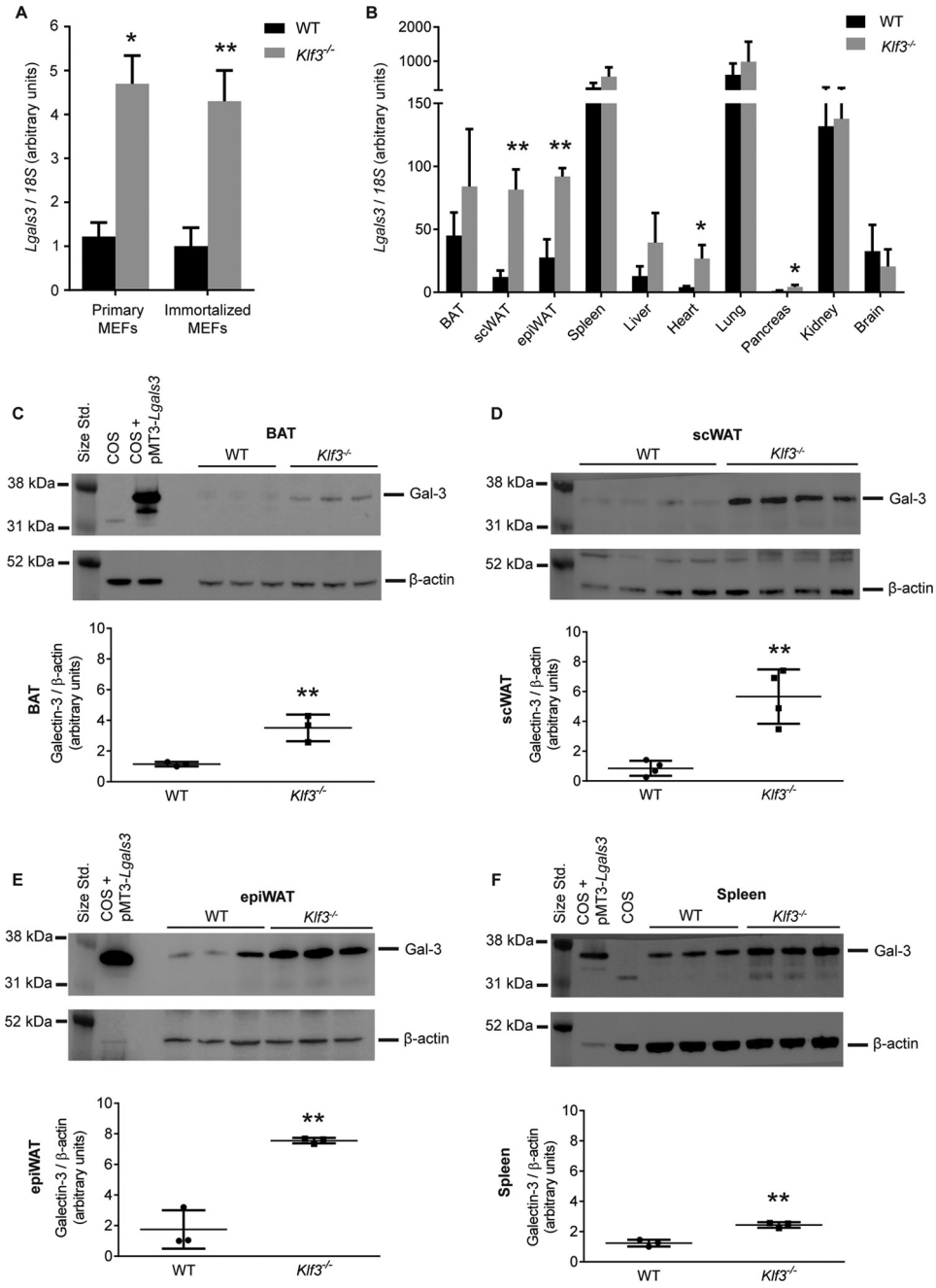

FIGURE 1. **Lgals3 is up-regulated in the absence of KLF3.** *A* and *B*, real-time quantitative PCR analysis of *Lgals3* mRNA levels in WT and *Klf3*$^{-/-}$ MEFs (*A*) and primary tissues (*B*). *Lgals3* expression was normalized with *18S* rRNA levels and normalized again to the condition with the lowest mean *Lgals3*/*18S* expression, which was set to 1 ($n = 3$ for *A* and $n = 4$–5 for *B*). *C*–*F*, Western blots showing galectin-3 protein expression in WT and *Klf3*$^{-/-}$ BAT (*C*), scWAT (*D*), epiWAT (*E*), and spleen (*F*) with densitometry analysis ($n = 3$–4). 15 μg of total protein was loaded per lane, alongside a Rainbow molecular weight marker (Amersham Biosciences) used as a protein size standard (*Size Std.*). Negative controls (nuclear extract from untransfected COS cells) and positive controls (nuclear extracts from COS cells expressing Gal-3) were included to show the expected migration pattern and test the specificity of the antibody for Gal-3. *Error bars* represent mean ± S.E., and Student's *t* tests were conducted to determine significance. *, $p < 0.05$; **, $p < 0.01$.

DNA probes corresponding to these motifs and evaluated direct protein binding by EMSA (Fig. 3*B*). KLF3 bound to each probe with the addition of an anti-KLF3 antibody, resulting in a supershift confirming the identity of probe-bound KLF3. The probes centered around −5 bp (Gal-3A) and −46 bp (Gal-3C) from the transcription start site displayed the most robust binding, suggesting that concurrent binding and dimerization of two KLF3 molecules at the promoter may occur given the spacing between these motifs, as has been postulated previously for other KLF3 target genes (14, 23). The middle site at −20 bp (Gal-3B) showed weaker binding.

Having established that KLF3 binds to motifs in the *Lgals3* proximal promoter, we next analyzed ChIP-seq data of genome-wide KLF3 binding in MEFs rescued with a tagged KLF3 cDNA transgene, KLF3-V5 (29), and found significant enrichment in and immediately upstream of the *Lgals3* gene (GEO accession no. GSE44748). Three significant peak clusters were identified: 19 kb upstream of the transcription start site

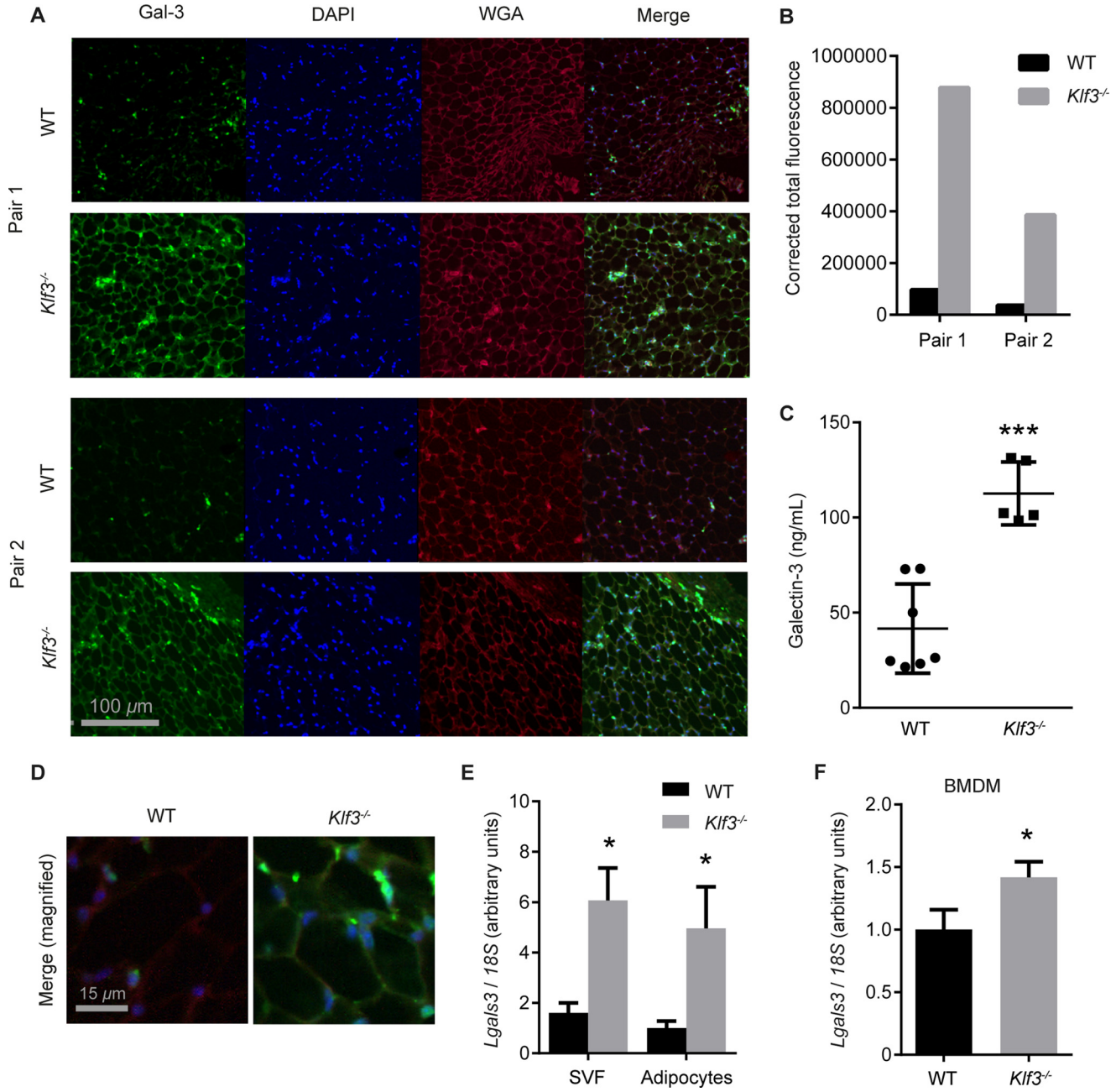

FIGURE 2. **Galectin-3 levels are elevated in *Klf3*$^{-/-}$ adipose tissue.** *A*, immunofluorescent staining of scWAT to assess galectin-3 levels, showing two representative WT and *Klf3*$^{-/-}$ pairs. DAPI and wheat germ agglutinin (*WGA*) were used to stain the nuclei and cell membranes, respectively. *B*, corrected total galectin-3 fluorescence using WT and *Klf3*$^{-/-}$ images from the Gal-3 column in *A*. *C*, levels of galectin-3 secreted after 2 h from WT and *Klf3*$^{-/-}$ epiWAT explants were measured using ELISA ($n = 7$ for WT and 5 for *Klf3*$^{-/-}$). *D*, the merged images from *A* were further magnified to assess galectin-3 up-regulation in adipocytes and the stromal vascular fraction of *Klf3*$^{-/-}$ scWAT. Up-regulation in both compartments of the scWAT was confirmed by real-time quantitative PCR analysis of *Lgals3* mRNA levels ($n = 3$) *E*, *Lgals3* levels were also assessed in cultured bone marrow-derived macrophages ($n = 4$). *SVF*, stromal vascular fraction. *F*, *Lgals3* expression was normalized with *18S* expression levels and normalized again to the condition with the lowest mean *Lgals3*/*18S* expression, which was set to 1. For *C*, *E*, and *F*, *error bars* represent mean ± S.E., and Student's *t* tests were conducted to determine significance. *, $p < 0.05$; ***, $p < 0.001$.

(site i), at the proximal promoter (site ii), and in the first intron (site iii) (Fig. 3*C*). These three prominent sites represent potential regulatory elements that are both accessible (as denoted by DNase-seq) and/or marked by active histone signatures (histone 3 lysine 4 trimethylation and histone 3 lysine 27 acetylation) in fibroblasts.

We also validated the ChIP-seq result with ChIP experiments followed by quantitative real-time PCR. Chromatin from wild-type and *Klf3*$^{-/-}$ MEFs was immunoprecipitated with an anti-KLF3 antibody and subjected to amplification using primers targeted to the −19 kb promoter and intron 1 ChIP-Seq peaks (sites i—iii, respectively) from Fig. 3*C*. Previously confirmed KLF3 binding sites at the *Fam132a* promoter and the *Klf8* promoter 1a were used as positive control loci, whereas primers targeting regions 30 kb downstream and 4.5 kb upstream of *Klf8* promoter 1a served as negative control regions A and B, respectively (14, 15). KLF3 enrichment at sites i, ii, and iii of *Lgals3* in WT cells was increased 4.5-, 10.7-, and 7.3-fold, respectively,

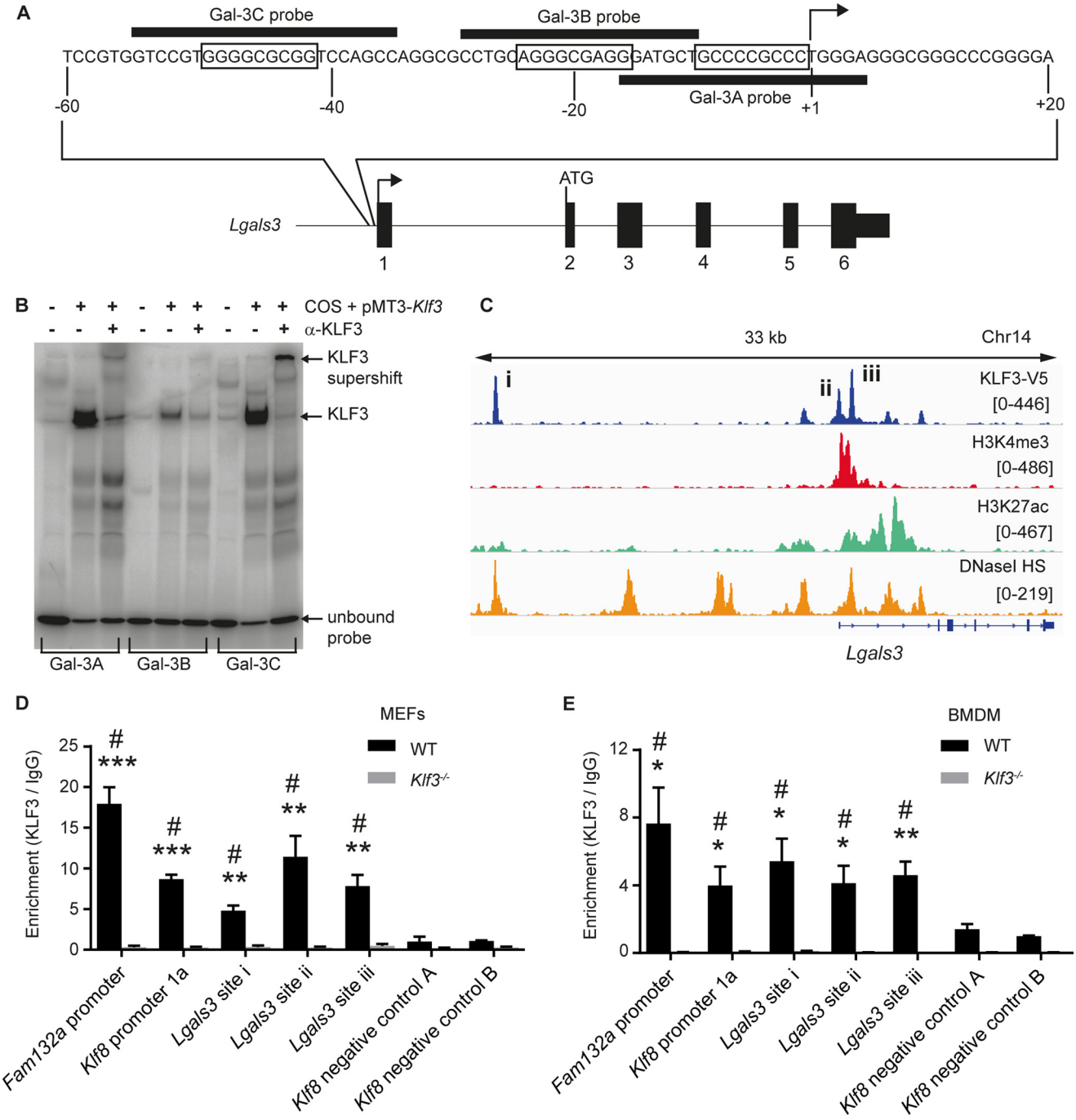

FIGURE 3. **KLF3 binds to the *Lgals3* promoter *in vitro* and *in vivo*.** *A*, *Lgals3* promoter region proximal to the transcription start site (+1) showing three KLF3 consensus binding sites (*boxed*) and their corresponding EMSA probes (Gal-3A, Gal-3B, and Gal-3C; *black bars*). The *Lgals3* sequence was derived from the mm9 *Mus musculus* genome (NCBI reference sequence NM_001145953). *B*, nuclear extracts were prepared from COS-7 cells transfected with 5 μg of pMT3-*Klf3*. These were used in EMSA to assess KLF3 binding of ^{32}P-radiolabeled probes Gal-3A, Gal-3B, and Gal-3C, each corresponding to KLF3 consensus motifs in the *Lgals3* proximal promoter from *A*. The addition of anti-KLF3 antibody was used to confirm the identity of the protein bound to the probes by supershift. *C*, KLF3 binding at *Lgals3* in MEFs from previously published KLF3-V5 ChIP-seq data available from GEO (accession# GSE44748) (29). KLF3 enrichment peaks are aligned with histone 3 lysine 4 trimethylation (accession no. GSM769029) and histone 3 lysine 27 acetylation (accession no. GSM1000139). ChIP-seq data from MEFs and a DNaseI hypersensitivity (accession no. GSM1014199) dataset were produced from murine fibroblasts (48–50). Significant KLF3 binding peaks at *Lgals3* are denoted by *i*, *ii*, and *iii*. *D* and *E*, *in vivo* occupancy of KLF3 at these sites (i, ii, and iii) in *Lgals3* was assessed in WT and *Klf3*$^{-/-}$ MEFs (*D*) and bone marrow-derived macrophages (*E*) ($n = 3$–4 for WT and 2–3 for *Klf3*$^{-/-}$). Sites i, ii, and iii from *C* were interrogated by quantitative PCR following chromatin immunoprecipitation with Pierce anti-KLF3 antibody (PA5-18030) or normal goat IgG. *Fam132a* and *Klf8* promoter 1a were used as positive control sites and *Klf8* negative controls A and B as negative control loci, as described previously (14, 15, 23). *Error bars* represent the mean ± S.E. Student's *t* tests were used to determine significance. *, $p < 0.05$; **, $p < 0.01$; ***$p < 0.001$; WT *versus* WT *Klf8*-negative control B (*D*) or *Klf8* negative control A (*E*). #, $p < 0.05$, WT *versus* *Klf3*$^{-/-}$ (*D* and *E*).

compared with the *Klf8* negative control B region (Fig. 3*D*). Negligible KLF3 enrichment was evident at any of the loci interrogated in *Klf3*$^{-/-}$ MEFs, confirming the specificity of the anti-KLF3 immunoprecipitation.

We extended this analysis to investigate the binding in bone marrow-derived macrophages. These cells were chosen as they are important in metabolism, and *Lgals3* is known to be a prominent macrophage marker (2, 30). Chromatin from WT and

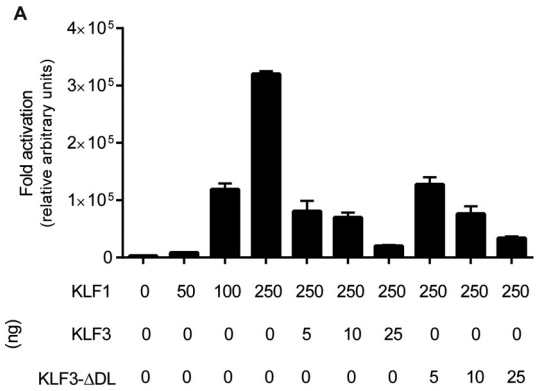

Condition 1	Condition 2	*p*-value
0 ng KLF1	50 ng KLF1	**0.006**
50 ng KLF1	100 ng KLF1	**0.002**
100 ng KLF1	250 ng KLF1	**0.000**
250 ng KLF1	5 ng KLF3	**0.001**
5 ng KLF3	10 ng KLF3	0.303
10 ng KLF3	25 ng KLF3	**0.003**
250 ng KLF1	5 ng KLF3-ΔDL	**0.001**
5 ng KLF3-ΔDL	10 ng KLF3-ΔDL	**0.024**
10 ng KLF3-ΔDL	25 ng KLF3-ΔDL	**0.017**
5 ng KLF3	5 ng KLF3-ΔDL	**0.049**
10 ng KLF3	10 ng KLF3-ΔDL	0.351
25 ng KLF3	25 ng KLF3-ΔDL	**0.008**

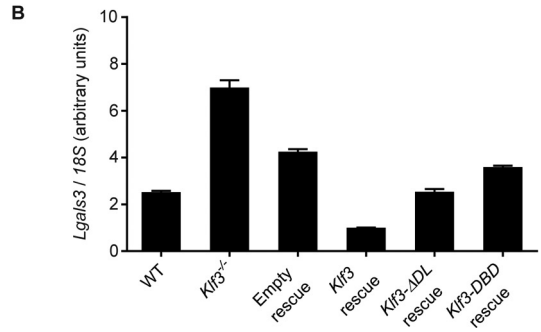

Condition 1	Condition 2	*p*-value
WT	*Klf3*$^{-/-}$	**0.0001**
Empty rescue	*Klf3* rescue	**0.000003**
Empty rescue	*Klf3-ΔDL* rescue	**0.0002**
Empty rescue	*Klf3-DBD* rescue	**0.003**
Klf3 rescue	*Klf3-ΔDL* rescue	**0.0001**
Klf3 rescue	*Klf3-DBD* rescue	**0.000001**
Klf3-ΔDL rescue	*Klf3-DBD* rescue	**0.0008**

FIGURE 4. **Optimal KLF3-mediated repression of *Lgals3* is partially dependent on CtBP and requires the KLF3 functional domain.** *A*, SL2 cells were transfected with 1 μg of pGL4.10[*luc2*] containing the core *Lgals3* promoter (−190 to +34, relative to the transcription start site). 1 μg of pGL4.74[*hRLuc*] was used as a transfection control. Empty pPac was added to assess transactivation in the absence of KLF1, KLF3, and KLF3-ΔDL, followed by addition of 50, 100, and 250 ng of pPac-*Klf1*. With activation of the construct driven by 250 ng of KLF1, increasing amounts of pPac-*Klf3* or pPac-*Klf3-ΔDL* were added to assess repression (5, 10, and 25 ng). The average of three replicates per condition is shown. *B*, real-time quantitative PCR analysis of *Lgals3* expression in WT, *Klf3*$^{-/-}$, and rescued *Klf3*$^{-/-}$ MEF cell lines ($n = 3$). *Error bars* represent the mean ± S.E., and Student's *t* tests were conducted to determine significance between conditions, shown in adjacent tables as *p* values ($p < 0.05$).

Klf3$^{-/-}$ macrophages was immunoprecipitated with anti-KLF3 antibody and then amplified by quantitative real-time PCR primers corresponding to the *Lgals3* sites i, ii, and iii from Fig. 3*C* to assess KLF3 occupancy (Fig. 3*E*). As in Fig. 3*D*, *Fam132a* and *Klf8* promoter 1a were used as positive control loci and *Klf8* negative control regions A and B as sites where KLF3 does not bind (23). The results in macrophages reflected those seen in MEFs, with strong enrichment evident at the −19 kb site (3.9-fold *versus Klf8* negative control A), the promoter (3-fold), and intron 1 (3.3-fold) of *Lgals3*, confirming KLF3 occupancy *in vivo* and indicating that KLF3 resides at *Lgals3* regulatory regions in multiple cell types, including primary cells.

KLF3 Repression of Lgals3 Involves Both CtBP-dependent and -independent Silencing—With the knowledge that KLF3 is able to bind consensus motifs in the *Lgals3* promoter and occupies this element *in vivo*, cellular reporter assays were undertaken in SL2 cells to determine whether KLF3 is able to directly repress *Lgals3* expression. Because of its reported role as a co-repressor for KLF3 (17), we investigated whether CtBP may be necessary for optimal silencing of *Lgals3* by testing the repressive capacity of a KLF3 mutant unable to bind CtBP (KLF3-ΔDL) (29). SL2 cells are typically used for analyzing the functional roles of KLF proteins because of the fact that, unlike mammalian cells, they lack endogenous CACCC-binding proteins that may interfere with assays (31). To examine repression, it was first necessary to activate the *Lgals3* promoter, and this was done by providing KLF1, a closely related activator of transcription that regulates a subset of KLF3 target genes and has been suggested to drive *Lgals3* expression (15).

We showed that increasing the dosage of KLF1 was sufficient to activate the reporter construct (Fig. 4*A*), and the 250-ng dosage was chosen as an optimal amount to drive expression and to determine what effect increasing doses of KLF3 has in competitive assays. In these, 0-, 5-, 10-, and 25-ng amounts of KLF3 or KLF3-ΔDL were added to cells containing the *Lgals3* promoter reporter construct. We have previously observed that the ΔDL mutation does not adversely affect the expression of KLF3 in SL2 cells (17). Addition of 5 ng of KLF3 was sufficient to significantly reduce *Lgals3* activation by 4-fold. 5 ng of KLF3-ΔDL also drove significant repression, but only 2.5-fold, suggesting the need for KLF3 to bind its co-repressor CtBP for effective silencing of *Lgals3*.

Given that the inability of KLF3 to bind CtBP resulted in impaired repression from our reporter assays, we sought to determine whether this affected *Lgals3* expression in a series of rescued *Klf3*$^{-/-}$ MEFs (Fig. 4*B*). *Klf3*$^{-/-}$ cells rescued with *Klf3-ΔDL* displayed 2.5-fold higher expression of *Lgals3* than cells rescued with wild type *Klf3*, confirming the observation from our reporter assays (Fig. 4*A*) that, without CtBP, KLF3 cannot optimally silence *Lgals3*. Furthermore, *Lgals3* expression in *Klf3*$^{-/-}$ cells rescued with the KLF3 DNA-binding domain only (*Klf3-DBD*) was 3.6-fold higher than those rescued with wild-type *Klf3* and only modestly reduced compared with empty vector-rescued cells. Together, these results demon-

strate that KLF3 binds to and is able to directly repress *Lgals3* expression and that elements in the KLF3 functional (non-DNA-binding) domain, including CtBP recruitment, are important for its capacity to silence target genes like *Lgals3*.

Discussion

Despite the importance of galectin-3 in a host of biological settings, little is known about how its gene is activated (32–34), and to our knowledge, there is no published work on the repression of *Lgals3*. Here we have shown that galectin-3 expression is up-regulated in the absence of KLF3, and we have demonstrated that KLF3 directly binds and represses the *Lgals3* promoter *in vivo*. Furthermore, we have provided mechanistic insights into KLF3 repression of *Lgals3*. In reporter assays, a KLF3 mutant that is unable to bind the co-repressor CtBP showed a reduced ability to repress *Lgals3*. Analysis of the expression levels of *Lgals3* in *Klf3*$^{-/-}$ MEFs rescued with KLF3 or a KLF3 mutant unable to bind to CtBP also showed that KLF3 recruitment of CtBP is necessary for optimal *Lgals3* repression. These two lines of evidence suggest that recruitment of the co-repressor CtBP is important for KLF3 repression of *Lgals3* but that CtBP-independent mechanisms also exist. We also assessed the contribution of the KLF3 functional domain to repression in *Klf3*$^{-/-}$ MEF rescue experiments. KLF3 DNA-binding domain only showed only a modest ability to rescue *Lgals3* repression when introduced into *Klf3*$^{-/-}$ MEFs, suggesting that the functional domain (where CtBP binds) is important and also that direct competition for DNA binding to the *Lgals3* promoter between KLF3 and the activating KLF1 is not likely to be a major feature of the mechanism of repression.

Galectin-3 has been identified as an important regulator of inflammation in metabolic tissues (27). Its deficiency in mice is associated with increased adiposity, systemic inflammation, and an accumulation of inflammatory cells in metabolic tissues (26, 28). This phenotype poses a striking contrast to that seen in mice lacking KLF3, which display reduced fat mass and are protected from diet-induced obesity and glucose intolerance (23). It has been proposed that the phenotype of KLF3-deficient mice may reflect the derepression of adipose tissue-derived hormones that regulate metabolism. For instance, we have reported that KLF3 represses the recently characterized adipokine adipolin (also known as Fam132a/CTRP12/C1qdc2) and suggested that the abundance of adipolin may in part explain the lean phenotype of KLF3-deficient mice (23). Given that galectin-3 has also been proposed to have a role in metabolism and is also derepressed in KLF3-deficient animals, it is possible that its up-regulation may also contribute to the KLF3 knockout mouse phenotype.

It is well established that obesity is accompanied by an accumulation of inflammatory immune cells, particularly macrophages, in adipose and other metabolic tissues (35, 36). Interestingly, galectin-3 appears to have both pro- and anti-inflammatory roles depending on the cellular and pathophysiological context. On the one hand, inhibition of galectin-3 in apolipoprotein E-deficient mice improves atherosclerotic progression (37). However galectin-3 has also been shown to bind and neutralize metabolic compounds known as advanced glycation end products, which arise from excessive nutrient accumulation and contribute to inflammation in type 2 diabetes (38). Elimination of advanced glycation end products protects tissue from sustained macrophage-mediated inflammatory signaling and associated metabolic complications, so galectin-3 is also regarded as a protective factor.

Elevated galectin-3 levels in adipose tissue lacking KLF3 may contribute to ameliorating the onset of chronic inflammation that might otherwise accompany obesity, insulin resistance, and glucose intolerance. It is notable that these metabolic complications do not develop in *Klf3*$^{-/-}$ mice even when they are maintained on a high-fat diet (23).

Additionally, we observed significant galectin-3 up-regulation in the pancreas of *Klf3*$^{-/-}$ mice, where galectin-3 has been shown to protect β cells from the inflammatory effects of interleukin 1β (8). We also found that *Lgals3* expression is elevated in *Klf3*$^{-/-}$ heart tissue, which may be important in the context of current research efforts focused on galectin-3 in cardiac function (5, 39). These findings necessitate further study to elucidate the role of KLF3 in the pancreas and heart, such as fibrotic progression and advanced glycation end product accumulation in *Klf3*$^{-/-}$ mice—areas that are presently lacking understanding.

Immunohistochemical staining of adipose sections from wild-type and *Klf3*$^{-/-}$ mice revealed that galectin-3 is highly up-regulated in both adipocytes and in cells of the stromal vascular compartment. Macrophages are an important component of this stromal fraction and are heavily implicated in the onset of chronic inflammation in obese adipose tissue (36). During this process, macrophages undergo a functional switch away from the alternatively activated state seen under normal conditions toward a more invasive and pro-inflammatory character, accompanied by changes in cellular metabolism (40). Interestingly, CtBP, which we have shown participates in KLF3-mediated repression of galectin-3, is known to act as a metabolic "sensor" through binding NADH, enhancing its propensity as a co-repressor (41, 42). This may be relevant to its role in silencing galectin-3 expression in macrophages undergoing metabolic remodeling toward a pro-inflammatory phenotype.

Galectin-3 is crucial in sustaining alternative activation in macrophages through an anti-inflammatory axis involving interleukin 4 and CD98 (2), protecting against the inflammatory shift that can contribute to insulin resistance and other metabolic complications. Up-regulation of galectin-3 in adipose tissue macrophages lacking KLF3 may convey anti-inflammatory benefits and, in part, account for the obesity-protected phenotype evident in *Klf3*$^{-/-}$ mice.

Accordingly, we investigated whether galectin-3 was regulated by KLF3 in macrophages themselves. We did observe binding of the KLF3 protein to *Lgals3* regulatory regions in ChIP experiments (Fig. 3*E*) and also observed some up-regulation of galectin-3 in *Klf3*$^{-/-}$ macrophages cultured from bone marrow (Fig. 2*F*). However, the up-regulation in macrophages was less striking than in other tissues, such as white adipose tissue and the heart. It remains to be determined whether this is a consequence of the fact that galectin-3 is already perhaps close to maximally expressed in wild-type murine macrophages. Indeed, galectin-3 was once known as Mac-2 because of

its high abundance as a macrophage surface marker (30). The full functional network controlling metabolism will involve both macrophages and other cells, including adipocytes, and further work will be required to determine the contributions of each cell type to the murine phenotypes.

In conclusion, we have demonstrated that KLF3 binds and represses *Lgals3*, regulating its expression *in vivo*. We have shown that optimal KLF3 repression of *Lgals3* is dependent on the functional domain of KLF3 and that both CtBP-dependent and CtBP-independent mechanisms are involved. Identification of *Lgals3* as a *bona fide* KLF3 target gene allows us to better understand how its expression is controlled. Given the well documented importance of galectin-3 in inflammation and other disease states, future considerations of how its expression is regulated may open up avenues for therapeutic intervention strategies.

Experimental Procedures

Mouse Generation and Genotyping—Generation of *Klf3*$^{-/-}$ mice on an FVB/NJ background and their genotyping have been reported previously (14, 24). Approval for the use of animals was from the University of Sydney Animal Care and Ethics Committee (protocol L02/7-2009/3/5054) and the University of New South Wales Animal Care and Ethics Committee (protocol 12/150A). Mice were weaned at 3 weeks and had *ad libitum* access to standard chow and water until sacrifice at 12 to 14 weeks of age.

Tissue Collection—12- to 14-week-old male mice were anesthetized with isoflurane and euthanized by cervical dislocation. Tissues were harvested promptly and washed with cold PBS and then frozen in RNAlater (Sigma). For fat depot collection, scWAT was harvested from the inguinal pads, visceral white adipose tissue from the epididymal depot (epiWAT), and BAT from the interscapular region. Femora and tibiae were kept on ice and immediately transferred to tissue culture for bone marrow lavage.

Collagenase Digestion of Fat—Inguinal scWAT was minced with scissors and then digested in 0.75 mg/ml type II collagenase (Sigma) for 45 min of shaking at 37 °C. The cell slurry was diluted in Hanks' buffered salt solution (Invitrogen) and then filtered through a prewet 100-μm mesh prior to separation of the stromal vascular fraction from adipocytes by centrifugation. Following red blood cell lysis in the stromal vascular fraction, both fractions were kept at −80 °C in preparation for RNA extraction.

Cell Culture—The wild-type, *Klf3*$^{-/-}$, and rescued *Klf3*$^{-/-}$ MEF cell lines used here have been described previously (29) and were cultured at 37 °C with 5% CO_2 in Dulbecco's modified Eagle's medium supplemented with 10% v/v heat-inactivated fetal calf serum and 1% v/v penicillin, streptomycin, and glutamine solution. COS-7 cells were cultured under the same conditions as MEFs. To generate macrophages, femora and tibiae from wild-type and *Klf3*$^{-/-}$ mice were flushed with cold phosphate-buffered saline, and bone marrow-derived macrophages (BMDM) were cultured over 7–10 days at 37 °C with 5% CO_2 in medium conditioned with M-CSF as described previously (43).

Secreted Galectin-3 Measurement from Adipose Explants—Approximately 50 mg of freshly excised epididymal adipose tissue from wild type and *Klf3*$^{-/-}$ mice was washed and incubated in 500 μl of pregassed (95% O_2, 5% CO_2) medium. Medium consisted of Krebs-Henseleit buffer (118.5 mM NaCl, 4.7 mM KCl, 1.2 mM KH_2PO_4, 25 mM $NaHCO_3$, 2.5 mM $CaCl_2{\cdot}2H_2O$, and 1.2 mM $MgSO_4{\cdot}7H_2O$) supplemented with 5 mM HEPES, 2% w/v bovine serum albumin (Sigma), and 5 mM glucose. Following 2 h of incubation, medium was collected for measurement of galectin-3 using the mouse galectin-3 ELISA kit (RayBiotech) according to the directions of the manufacturer.

Protein Extraction and Western Blotting—Whole cell extracts were prepared in radioimmune precipitation assay buffer (50 mM HEPES (pH 7.5), 500 mM LiCl, 1 mM EDTA, 1% Nonidet P-40, and 0.7% sodium deoxycholate) with protease inhibitors from 20-mg portions of epiWAT, scWAT, BAT, and spleen. Total protein levels were assessed using a bicinchoninic acid protein assay (ThermoFisher). For control lanes, COS-7 cells were transfected with pMT3-*Lgals3* using FuGENE6 (Promega) or left untransfected and then harvested 48 h later for nuclear extraction as described previously (16). Western blotting was performed according to standard methods. In brief, 15 μg of protein was separated by SDS-PAGE and transferred to a nitrocellulose membrane, which was blocked with 3.5% skim milk in 50 mM Tris-HCl (pH 7.4), 150 mM NaCl, and 0.05% Tween 20 (TBST). Membranes were probed for galectin-3 and β-actin protein for 1 h at room temperature in TBST with anti-galectin-3 (AF1197, R&D Systems) and anti-β-actin (A1978, Sigma) antibodies. The Immobilon Western chemiluminescent HRP substrate system (Millipore Corp.) was used for detection. ImageJ was used for densitometry quantification of Western blotting bands, where three background areas were used to normalize galectin-3 and β-actin band intensity.

RNA Extraction and cDNA Synthesis—MEFs and bone marrow-derived macrophages were harvested at 95% confluency, and total RNA was extracted using the RNeasy mini kit (Qiagen). The DNA-free kit (Ambion) was used to eliminate genomic DNA contamination. Tissues were harvested and suspended in TRI reagent (Sigma) or QIAzol lysis reagent (Qiagen) for lipid-rich adipose and brain samples. A TissueLyser II (Qiagen) was used to disrupt and homogenize tissues before extraction of RNA using the RNeasy mini or lipid tissue mini kit (Qiagen) according to the instructions of the manufacturer. For RNA extraction from stromal vascular and adipocyte fractions of scWAT, the RNeasy Plus mini kit (Qiagen) was utilized because of lower initial sample quantity. Residual genomic DNA was eliminated by treatment with the RNase-free DNase kit (Qiagen) prior to cDNA synthesis. RNA was converted into cDNA with the SuperScript VILO cDNA synthesis kit (Invitrogen) for use in quantitative real-time PCR.

Quantitative Real-time PCR and Primer Design—Primers were designed as described previously (44). The oligonucleotide sequences were as follows: *18S*, 5′-CACGGCCGGTACAGTGAAAC-3′ and 5′-AGAGGAGCGAGCGACCAA-3′; *Lgals3*, 5′-GATCACAATCATGGGCACAG-3′ and 5′-ATTGAAGCGGGGGTTAAAGT-3′. Quantitative real-time PCR runs were performed in triplicate with Power SYBR Green PCR

Master Mix and the 7500 fast real-time PCR system (Applied Biosystems) as described previously (45).

Immunohistochemistry—Inguinal scWAT was harvested from 12- to 14-week-old male wild-type and *Klf3*$^{-/-}$ mice, and portions were fixed overnight in 4% buffered formalin prior to paraffin embedding. 8-μm sections of tissue were rehydrated with xylene and graded ethanol before treatment with citrate buffer, a heat-induced antigen retriever. Following this, sections were incubated with 2% w/v skim milk to block nonspecific background staining. The sections were then incubated for 90 min with primary goat anti-galectin-3 (AF1197, R&D Systems). Subsequently, a 45-min incubation was undertaken with secondary donkey anti-goat IgG conjugated to Alexa Fluor 488 (A-11055, ThermoFisher) as well as Alexa Fluor 633-conjugated wheat germ agglutinin (W21404, ThermoFisher) before treatment with 0.1% v/v Sudan black B to reduce autofluorescence. Stained sections were rinsed, and a DAPI coverslip was applied prior to imaging. Images were captured at ×20 magnification using a ScanScope FL (Aperio Technologies), and scanned slides were visualized with ImageScope software (Aperio Technologies). ImageJ was used to calculate the corrected total fluorescence of galectin-3 using a method described previously (46) by subtracting the selected area size times the average background fluorescence from the integrated density. Three areas of interest and background regions were randomly selected per section.

EMSA—COS-7 cells were transfected with pMT3-*Klf3* using FuGENE6 (Promega) and harvested 48 h later for nuclear extraction and EMSA, performed as described previously (16). For detection of KLF3 binding, equal quantities of nuclear extracts were loaded with radiolabeled probes in a total volume of 30 μl containing 50 μg/ml poly(dI-dC), 4.4 mM dithiothreitol, 100 μg/ml bovine serum albumin, 10 mM HEPES (pH 7.8), 50 mM KCl, 5 mM $MgCl_2$, 1.33 mM $MnCl_2$, 3.33 mM NaCl, 35 mM Tris-HCl (pH 7.5), 3.33 μM EGTA, 1.07 mM EDTA, 0.007% Brij35, 6.67% glycerol, and 1 μl of anti-KLF3 antibody or rabbit preimmune serum as appropriate. Generation of the anti-KLF3 antibody has been described previously (16). Three oligonucleotide probes were designed, corresponding to KLF3 binding motifs found in the *Lgals3* proximal promoter (Fig. 3*B*) and radiolabeled using ^{32}P. The probe sequences were as follows: Gal-3A, 5′-GATGCTGCCCCGCCCTGGGAG-3′ and 5′-CTCCCAGGGCGGGGCAGCATC-3′; Gal-3B, 5′-CCTGCAGGGCGAGGGATGCTG-3′ and 5′-CAGCATCCCTCGCCCTGCAGG-3′; and Gal-3C, 5′-TCCGTGGGGCGCGGTCCAGCC-3′ and 5′-GGCTGGACCGCGCCCCACGGA-3′.

ChIP and Quantitative Real-time PCR—ChIP was performed on wild-type and *Klf3*$^{-/-}$ MEFs and BMDM according to precedent (47). Approximately 5 × 10^7 cells/experiment were grown to 95% confluence, fixed with 1% formaldehyde for 10 min, and quenched with 2.5 M glycine. BMDM were stimulated with 100 ng/ml lipopolysaccharide (Sigma) for 4 h before fixing. Sonication of chromatin was achieved using a Biorupter (Diagenode) on a 30 s on/30 s off cycle for 15 min (MEFs) or 3 × 10 min (BMDM). DNA was subsequently immunoprecipitated with either the Pierce anti-KLF3 antibody (PA5–18030) or normal goat IgG (SC-2028). Immunoprecipitated DNA was analyzed by quantitative real-time PCR using the following primers: *Klf8* promoter 1a, 5′-CCAGCTCGTGCACACTGAA-3′ and 5′-GAAGCCTTAACATCAGGAGTGGAA-3′; *Klf8* negative control A (30 kb downstream of *Klf8* promoter 1a), 5′-AACCTGGGTGCCTCCTTGTA-3′ and 5′-TCATGCCTTTGACTTTAG-TGCTTT-3′; *Klf8* negative control B (4.5 kb upstream of *Klf8* promoter 1a), 5′-GGTTTCTGAGACCTAACACTTCACACT-3′ and 5′-CCATTTAGTCATCCAGCGAACAA-3′; *Fam132a* promoter, 5′-GATTCGCTTCCCTGGAGGTGTGG-3′ and 5′-GCCCAG-TCTCTGGTCTCCTCTCT-3′; *Lgals3* site i (19 kb upstream of promoter), 5′-TGGAAAAACACCCGTGCCTCTGA-3′ and 5′-CAGTGCCTACGCCCAGATGACTC-3′; *Lgals3* site ii (promoter), 5′-GAGCAGGAGTGAATGCAAACAG-3′ and 5′-GCAGAAATGGCAGTGACTTTGA-3′; and *Lgals3* site iii (intron 1), 5′-TCGTGACCAGTGTGGTTATTTGT-3′ and 5′-TCTCGCTAAGGGTCTGCACTCT-3′.

Vectors and Cloning of the Lgals3 Promoter—The *Lgals3* promoter region spanning from −190 to +34 *bp* relative to the transcription start site was amplified from wild-type FVB/NJ murine genomic DNA by PCR using the forward primer 5′-ATTAGGTACCGACAGGCAGCTTCAGACA-3′ and the reverse primer 5′-ATTACTCGAGCTTCTAGTACTCTTTTCCCCG-3′. This region was subcloned into KpnI/XhoI pGL4.10[*luc2*] (Promega) to generate pGL4.10[*luc2*]-*Lgals3*-prom(−190 + 34). pPac and pPac-*Klf1* were kindly provided by Menie Merika and Stuart Orkin (Harvard Medical School, Boston, MA), whereas pPac-*Klf3* and pPac-*Klf3*-Δ*DL* were supplied by José Perdomo (School of Molecular Bioscience, Sydney, NSW, Australia).

Reporter Assays—SL2 cells were seeded in 6-well plates at a concentration of 1 × 10^6/ml in preparation for transfection using FuGENE6 (Promega). 24 h later, cells were transfected with pPac-*Klf1* (0, 50, 100, or 250 ng) supplemented with the empty pPac vector for equal loading as well as 100 ng of pGL4.74[*hRLuc*] and 1 μg of pGL4.10[*luc2*]-*Lgals3*prom (−190 + 34). For repression assays, activation was driven by 250 ng of pPac-*Klf1* and increasing dosages of pPac-*Klf3* or pPac-*Klf3*-Δ*DL* added (0, 5, 10, and 25 ng). Cells were harvested 48 h later, and lysates were analyzed using the Dual-Luciferase reporter assay system (Promega) according to the instructions of the manufacturer.

ChIP- and DNase-seq Datasets—A ChIP-seq dataset for V5-tagged KLF3 produced from murine embryonic fibroblasts was used to assess genome-wide KLF3 binding and was obtained from GEO (accession no. GSE44748) (29). ENCODE datasets for genome-wide histone 3 lysine 4 trimethylation and histone 3 lysine 27 acetylation were produced from murine embryonic fibroblasts by the Ren laboratory at the Ludwig Institute for Cancer Research. Both were downloaded from GEO (accession nos. GSM769029 and GSM1000139, respectively) (48, 49). A DNase-seq dataset produced from murine fibroblasts by the Stamatoyannopoulos laboratory at the University of Washington was also downloaded from GEO (accession no. GSM1014199) (48, 50).

Statistical Analysis—Data are presented as mean ± S.E. Significance was determined using Student's *t* tests, with $p < 0.05$ being taken as statistically significant.

Author Contributions—A. J. K., K. G. R. Q., and M. C. wrote the manuscript with comments from all authors. A. J. K., J. J. Y., H. M. J., and L. J. N. performed the experiments. A. J. K., A. P. W. F., R. C. M. P., M. C., and K. G. R. Q. designed the study. K. S. B. A. provided tissue material, training, and experimental support. All authors reviewed the results and approved the final version of the manuscript.

Acknowledgments—We thank Ka Sin Mak for help with technical training and mouse work. We also acknowledge the Histology and Microscopy Unit at the University of New South Wales for immunohistochemistry services and guidance.

References

1. Dagher, S. F., Wang, J. L., and Patterson, R. J. (1995) Identification of galectin-3 as a factor in pre-mRNA splicing. *Proc. Natl. Acad. Sci. U.S.A.* **92,** 1213–1217
2. MacKinnon, A. C., Farnworth, S. L., Hodkinson, P. S., Henderson, N. C., Atkinson, K. M., Leffler, H., Nilsson, U. J., Haslett, C., Forbes, S. J., and Sethi, T. (2008) Regulation of alternative macrophage activation by galectin-3. *J. Immunol.* **180,** 2650–2658
3. Elad-Sfadia, G., Haklai, R., Balan, E., and Kloog, Y. (2004) Galectin-3 augments K-Ras activation and triggers a Ras signal that attenuates ERK but not phosphoinositide 3-kinase activity. *J. Biol. Chem.* **279,** 34922–34930
4. Yang, R. Y., Hsu, D. K., and Liu, F. T. (1996) Expression of galectin-3 modulates T-cell growth and apoptosis. *Proc. Natl. Acad. Sci. U.S.A.* **93,** 6737–6742
5. de Boer, R. A., Voors, A. A., Muntendam, P., van Gilst, W. H., and van Veldhuisen, D. J. (2009) Galectin-3: a novel mediator of heart failure development and progression. *Eur. J. Heart Fail.* **11,** 811–817
6. Henderson, N. C., Mackinnon, A. C., Farnworth, S. L., Poirier, F., Russo, F. P., Iredale, J. P., Haslett, C., Simpson, K. J., and Sethi, T. (2006) Galectin-3 regulates myofibroblast activation and hepatic fibrosis. *Proc. Natl. Acad. Sci. U.S.A.* **103,** 5060–5065
7. Srivatsan, V., George, M., and Shanmugam, E. (2015) Utility of galectin-3 as a prognostic biomarker in heart failure: where do we stand? *Eur. J. Prev. Cardiol.* **22,** 1096–1110
8. Karlsen, A. E., Størling, Z. M., Sparre, T., Larsen, M. R., Mahmood, A., Størling, J., Roepstorff, P., Wrzesinski, K., Larsen, P. M., Fey, S., Nielsen, K., Heding, P., Ricordi, C., Johannesen, J., Kristiansen, O. P., *et al.* (2006) Immune-mediated beta-cell destruction in vitro and in vivo-A pivotal role for galectin-3. *Biochem. Biophys. Res. Commun.* **344,** 406–415
9. Iacobini, C., Menini, S., Oddi, G., Ricci, C., Amadio, L., Pricci, F., Olivieri, A., Sorcini, M., Di Mario, U., Pesce, C., and Pugliese, G. (2004) Galectin-3/AGE-receptor 3 knockout mice show accelerated AGE-induced glomerular injury: evidence for a protective role of galectin-3 as an AGE receptor. *FASEB J.* **18,** 1773–1775
10. Pearson, R., Fleetwood, J., Eaton, S., Crossley, M., and Bao, S. (2008) Kruppel-like transcription factors: a functional family. *Int. J. Biochem. Cell Biol.* **40,** 1996–2001
11. Pearson, R. C., Funnell, A. P., and Crossley, M. (2011) The mammalian zinc finger transcription factor Kruppel-like factor 3 (KLF3/BKLF). *IUBMB Life* **63,** 86–93
12. Kaushik, D. K., Gupta, M., Das, S., and Basu, A. (2010) Kruppel-like factor 4, a novel transcription factor regulates microglial activation and subsequent neuroinflammation. *J. Neuroinflammation* **7,** 68
13. Rowland, B. D., Bernards, R., and Peeper, D. S. (2005) The KLF4 tumour suppressor is a transcriptional repressor of p53 that acts as a context-dependent oncogene. *Nat. Cell Biol.* **7,** 1074–1082
14. Eaton, S. A., Funnell, A. P., Sue, N., Nicholas, H., Pearson, R. C., and Crossley, M. (2008) A network of Kruppel-like Factors (Klfs). Klf8 is repressed by Klf3 and activated by Klf1 *in vivo*. *J. Biol. Chem.* **283,** 26937–26947
15. Funnell, A. P., Norton, L. J., Mak, K. S., Burdach, J., Artuz, C. M., Twine, N. A., Wilkins, M. R., Power, C. A., Hung, T. T., Perdomo, J., Koh, P., Bell-Anderson, K. S., Orkin, S. H., Fraser, S. T., Perkins, A. C., *et al.* (2012) The CACCC-binding protein KLF3/BKLF represses a subset of KLF1/EKLF target genes and is required for proper erythroid maturation *in vivo*. *Mol. Cell. Biol.* **32,** 3281–3292
16. Crossley, M., Whitelaw, E., Perkins, A., Williams, G., Fujiwara, Y., and Orkin, S. H. (1996) Isolation and characterization of the cDNA encoding BKLF/TEF-2, a major CACCC-box-binding protein in erythroid cells and selected other cells. *Mol. Cell. Biol.* **16,** 1695–1705
17. Turner, J., and Crossley, M. (1998) Cloning and characterization of mCtBP2, a co-repressor that associates with basic Kruppel-like factor and other mammalian transcriptional regulators. *EMBO J.* **17,** 5129–5140
18. Shi, Y., Sawada, J., Sui, G., Affar el, B., Whetstine, J. R., Lan, F., Ogawa, H., Luke, M. P., Nakatani, Y., and Shi, Y. (2003) Coordinated histone modifications mediated by a CtBP co-repressor complex. *Nature* **422,** 735–738
19. Ueda, J., Tachibana, M., Ikura, T., and Shinkai, Y. (2006) Zinc finger protein Wiz links G9a/GLP histone methyltransferases to the co-repressor molecule CtBP. *J. Biol. Chem.* **281,** 20120–20128
20. Dewi, V., Kwok, A., Lee, S., Lee, M. M., Tan, Y. M., Nicholas, H. R., Isono, K., Wienert, B., Mak, K. S., Knights, A. J., Quinlan, K. G., Cordwell, S. J., Funnell, A. P., Pearson, R. C., and Crossley, M. (2015) Phosphorylation of Kruppel-like factor 3 (KLF3/BKLF) and C-terminal binding protein 2 (CtBP2) by homeodomain-interacting protein kinase 2 (HIPK2) modulates KLF3 DNA binding and activity. *J. Biol. Chem.* **290,** 8591–8605
21. Perdomo, J., Verger, A., Turner, J., and Crossley, M. (2005) Role for SUMO modification in facilitating transcriptional repression by BKLF. *Mol. Cell. Biol.* **25,** 1549–1559
22. Vu, T. T., Gatto, D., Turner, V., Funnell, A. P., Mak, K. S., Norton, L. J., Kaplan, W., Cowley, M. J., Agenès, F., Kirberg, J., Brink, R., Pearson, R. C., and Crossley, M. (2011) Impaired B cell development in the absence of Kruppel-like factor 3. *J. Immunol.* **187,** 5032–5042
23. Bell-Anderson, K. S., Funnell, A. P., Williams, H., Mat Jusoh, H., Scully, T., Lim, W. F., Burdach, J. G., Mak, K. S., Knights, A. J., Hoy, A. J., Nicholas, H. R., Sainsbury, A., Turner, N., Pearson, R. C., and Crossley, M. (2013) Loss of Kruppel-like factor 3 (KLF3/BKLF) leads to upregulation of the insulin-sensitizing factor adipolin (FAM132A/CTRP12/C1qdc2). *Diabetes* **62,** 2728–2737
24. Sue, N., Jack, B. H., Eaton, S. A., Pearson, R. C., Funnell, A. P., Turner, J., Czolij, R., Denyer, G., Bao, S., Molero-Navajas, J. C., Perkins, A., Fujiwara, Y., Orkin, S. H., Bell-Anderson, K., and Crossley, M. (2008) Targeted disruption of the basic Kruppel-like factor gene (Klf3) reveals a role in adipogenesis. *Mol. Cell. Biol.* **28,** 3967–3978
25. Kelsey, L., Flenniken, A. M., Qu, D., Funnell, A. P., Pearson, R., Zhou, Y. Q., Voronina, I., Berberovic, Z., Wood, G., Newbigging, S., Weiss, E. S., Wong, M., Quach, I., Yeh, S. Y., Deshwar, A. R., *et al.* (2013) ENU-induced mutation in the DNA-binding domain of KLF3 reveals important roles for KLF3 in cardiovascular development and function in mice. *PLoS Genet.* 10.1371/journal.pgen.1003612
26. Pang, J., Rhodes, D. H., Pini, M., Akasheh, R. T., Castellanos, K. J., Cabay, R. J., Cooper, D., Perretti, M., and Fantuzzi, G. (2013) Increased adiposity, dysregulated glucose metabolism and systemic inflammation in Galectin-3 KO mice. *PLoS ONE* 10.1371/journal.pone.0057915
27. Pejnovic, N. N., Pantic, J. M., Jovanovic, I. P., Radosavljevic, G. D., Djukic, A. L., Arsenijevic, N. N., and Lukic, M. L. (2013) Galectin-3 is a regulator of metaflammation in adipose tissue and pancreatic islets. *Adipocyte* **2,** 266–271
28. Pejnovic, N. N., Pantic, J. M., Jovanovic, I. P., Radosavljevic, G. D., Milovanovic, M. Z., Nikolic, I. G., Zdravkovic, N. S., Djukic, A. L., Arsenijevic, N. N., and Lukic, M. L. (2013) Galectin-3 deficiency accelerates high-fat diet-induced obesity and amplifies inflammation in adipose tissue and pancreatic islets. *Diabetes* **62,** 1932–1944
29. Burdach, J., Funnell, A. P., Mak, K. S., Artuz, C. M., Wienert, B., Lim, W. F., Tan, L. Y., Pearson, R. C., and Crossley, M. (2014) Regions outside the DNA-binding domain are critical for proper *in vivo* specificity of an archetypal zinc finger transcription factor. *Nucleic Acids Res.* **42,** 276–289
30. Ho, M. K., and Springer, T. A. (1982) Mac-2, a novel 32,000 Mr mouse macrophage subpopulation-specific antigen defined by monoclonal antibodies. *J. Immunol.* **128,** 1221–1228
31. Courey, A. J., and Tjian, R. (1988) Analysis of Sp1 *in vivo* reveals multiple

transcriptional domains, including a novel glutamine-rich activation motif. *Cell* **55,** 887–898
32. Stock, M., Schäfer, H., Stricker, S., Gross, G., Mundlos, S., and Otto, F. (2003) Expression of galectin-3 in skeletal tissues is controlled by Runx2. *J. Biol. Chem.* **278,** 17360–17367
33. Vladimirova, V., Waha, A., Lückerath, K., Pesheva, P., and Probstmeier, R. (2008) Runx2 is expressed in human glioma cells and mediates the expression of galectin-3. *J. Neurosci. Res.* **86,** 2450–2461
34. Zhang, H. Y., Jin, L., Stilling, G. A., Ruebel, K. H., Coonse, K., Tanizaki, Y., Raz, A., and Lloyd, R. V. (2009) RUNX1 and RUNX2 upregulate Galectin-3 expression in human pituitary tumors. *Endocrine* **35,** 101–111
35. Chawla, A., Nguyen, K. D., and Goh, Y. P. (2011) Macrophage-mediated inflammation in metabolic disease. *Nat. Rev. Immunol.* **11,** 738–749
36. Lumeng, C. N., Bodzin, J. L., and Saltiel, A. R. (2007) Obesity induces a phenotypic switch in adipose tissue macrophage polarization. *J. Clin. Invest.* **117,** 175–184
37. MacKinnon, A. C., Liu, X., Hadoke, P. W., Miller, M. R., Newby, D. E., and Sethi, T. (2013) Inhibition of galectin-3 reduces atherosclerosis in apolipoprotein E-deficient mice. *Glycobiology* **23,** 654–663
38. Brownlee, M. (1995) Advanced protein glycosylation in diabetes and aging. *Annu. Rev. Med.* **46,** 223–234
39. Ahmad, T., and Felker, G. M. (2012) Galectin-3 in heart failure: more answers or more questions? *J. Am. Heart. Assoc.* 10.1161/JAHA.112.004374
40. Kelly, B., and O'Neill, L. A. (2015) Metabolic reprogramming in macrophages and dendritic cells in innate immunity. *Cell Res.* **25,** 771–784
41. Fjeld, C. C., Birdsong, W. T., and Goodman, R. H. (2003) Differential binding of NAD^+ and NADH allows the transcriptional corepressor carboxyl-terminal binding protein to serve as a metabolic sensor. *Proc. Natl. Acad. Sci. U.S.A.* **100,** 9202–9207
42. Jack, B. H., Pearson, R. C., and Crossley, M. (2011) C-terminal binding protein: a metabolic sensor implicated in regulating adipogenesis. *Int. J. Biochem. Cell Biol.* **43,** 693–696
43. Zhang, X., Goncalves, R., and Mosser, D. M. (2008) The isolation and characterization of murine macrophages. *Curr. Protoc. Immunol.* **83,** 14.1.1–14.1.14
44. Funnell, A. P., Maloney, C. A., Thompson, L. J., Keys, J., Tallack, M., Perkins, A. C., and Crossley, M. (2007) Erythroid Kruppel-like factor directly activates the basic Kruppel-like factor gene in erythroid cells. *Mol. Cell. Biol.* **27,** 2777–2790
45. Hancock, D., Funnell, A., Jack, B., and Johnston, J. (2010) Introducing undergraduate students to real-time PCR. *Biochem. Mol. Biol. Educ.* **38,** 309–316
46. McCloy, R. A., Rogers, S., Caldon, C. E., Lorca, T., Castro, A., and Burgess, A. (2014) Partial inhibition of Cdk1 in G 2 phase overrides the SAC and decouples mitotic events. *Cell Cycle* **13,** 1400–1412
47. Schmidt, D., Wilson, M. D., Spyrou, C., Brown, G. D., Hadfield, J., and Odom, D. T. (2009) ChIP-seq: using high-throughput sequencing to discover protein-DNA interactions. *Methods* **48,** 240–248
48. Encode Project Consortium. (2011) A user's guide to the encyclopedia of DNA elements (ENCODE). *PLoS Biol.* 10.1371/journal.pbio.1001046
49. Shen, Y., Yue, F., McCleary, D. F., Ye, Z., Edsall, L., Kuan, S., Wagner, U., Dixon, J., Lee, L., Lobanenkov, V. V., and Ren, B. (2012) A map of the cis-regulatory sequences in the mouse genome. *Nature* **488,** 116–120
50. Neph, S., Stergachis, A. B., Reynolds, A., Sandstrom, R., Borenstein, E., and Stamatoyannopoulos, J. A. (2012) Circuitry and dynamics of human transcription factor regulatory networks. *Cell* **150,** 1274–1286